

## DECOMPOSITION KINETICS OF AMERICAN, CHINESE AND ESTONIAN OIL SHALES KEROGEN

BIRGIT MAATEN<sup>(a)\*</sup>, LAURI LOO<sup>(a)</sup>, ALAR KONIST<sup>(a,b)</sup>,  
DMITRI NEŠUMAJEV<sup>(a)</sup>, TÕNU PIHU<sup>(a)</sup>,  
INDREK KÜLAOTS<sup>(a,b)</sup>

<sup>(a)</sup> Department of Thermal Engineering, Tallinn University of Technology, Ehitajate tee 5, 19086 Tallinn, Estonia

<sup>(b)</sup> School of Engineering, Brown University, 184 Hope Street, Providence, Rhode Island 02912, United States

**Abstract.** *An investigation of the pyrolysis kinetics of American, Chinese and Estonian oil shales was conducted applying a non-isothermal thermogravimetric analysis (TGA). TGA weight loss curves clearly indicate that the pyrolysis of all oil shales tested is independent of their geographic origin, and is mainly taking place in the temperature range of 300 to 500 °C. As expected, at temperatures above 700 °C mass loss due to the decomposition of oil shale carbonates was detected, except for the Kentucky and Chinese 2 oil shale samples. The kinetic decomposition rate parameters such as activation energy and pre-exponential factor were calculated applying the Coats-Redfern integral and direct Arrhenius methods. Independent of the oil shale kerogen origin, pyrolysis occurs in two consecutive temperature zones with slightly dissimilar kinetic parameter values. The activation energy values obtained were in the range of 14 to 31 kJ/mol for the low and 70 to 149 kJ/mol for the high temperature zone.*

**Keywords:** *oil shale decomposition kinetics, kerogen, pyrolysis, reaction rate, pre-exponential factor, activation energy.*

### 1. Introduction

Oil shale, a sedimentary rock found in many regions of the world, is largely used as a fossil fuel to generate electrical energy or higher value fuels. More than 600 deposits are known all over the world [1], the most vast ones of which are found in U.S.A., China, Brazil and Estonia [2]. Oil shale offers a reasonable alternative to conventional energy resources such as crude oil, coal and natural gas. Estonia has large resources of oil shale and today,

---

\* Corresponding author: e-mail [birgit.maaten@ttu.ee](mailto:birgit.maaten@ttu.ee)

approximately 90% of the country's electricity is produced in thermal power plants operating on oil shale as fuel [1, 3]. Oil shale consists of an insoluble organic part called kerogen and of a rich inorganic part, which consists mostly of a wide selection of mineral components (quartz, calcite, dolomite, etc.) [4]. The kerogen part has a complex cross-linked structure and high molecular weight up to 3000 [5]. For example, the kerogen from Estonian oil shale has the dominating functionalities of alcohols, ketones, amines and ethers, and also long aliphatic chains [6]. Compared to oil shale found in different countries, Estonian oil shale has a relatively high content of carbonate minerals [2]. The organic part has a relatively high content of hydrogen – the atomic ratio of H/C is 1.4–1.5 and the atomic ratio of O/C is 0.16–0.2 [2], which makes it hard to distinguish between Type I and Type II kerogens [7]. In comparison, the oil shale from Colorado, U.S.A., which originates from the Eocene age, has an organic carbon content of only 11–16%. The oil shale from Maoming, China, is known to have an organic carbon content of about 14% [8].

During pyrolysis upon heating in an inert atmosphere oil shale kerogen is first converted into a viscous mixture of hydrocarbons called bitumen, and then into final products such as shale oil (a mixture of shorter length hydrocarbons). The byproduct of the process is solid carbon rich oil shale semicoke [9]. Due to the complex structure of kerogen, several bonds are broken during the pyrolysis process, leading to multiple reactions [10]. Beside the oil shale thermal treatment, solvent extraction techniques can be used to extract shale oil from oil shale. The downside of the solvent extraction technique is that it requires solvents that are harmful to the environment and are problematic or expensive to use in the industry on a large scale [11].

Oil shale pyrolysis consists of three main processes: 1) water evaporation at lower temperatures (below 200 °C), 2) pyrolysis of kerogen (from 200 up to 600 °C), and 3) decomposition of carbonates (at temperatures above 700 °C) [12, 13]. Normally the pyrolysis process is studied in an inert atmosphere, for example such as N<sub>2</sub> gas, thereby avoiding the oxidation of the sample. There are numerous studies on the thermal decomposition and kinetic calculations of various oil shale samples available in the literature and therefore, several decomposition kinetic rate models have been suggested [12, 14–16]. The majority of those kinetic models consider kerogen decomposition in the pyrolysis process as a first order reaction. Previous research has shown that changing the carrier gas from N<sub>2</sub> to CO<sub>2</sub> does not considerably change the total weight loss or the mechanism of kerogen decomposition, since the oil shale semicoke's carbon oxidation in CO<sub>2</sub> occurs at way higher temperatures. In addition, the decomposition of carbonates in oil shale is reported to be retarded in CO<sub>2</sub> environment [17].

Thermogravimetric apparatus (TGA) is a widely used instrument to analyze the kinetics of thermal decomposition of various solids and liquids because of its clear advantages – ability to set a defined atmosphere and apply a wide range of heating rates. When TGA operates together with the

differential scanning calorimeter (DSC), the resulting reaction thermal effects can be identified and quantified. From the TGA raw data one can calculate kinetic rate parameters for the reaction by applying the existing theoretical model [18]. Isothermal and non-isothermal TGA approaches have been widely used to study oil shale thermal behavior [11, 13, 19–21] in various conditions. Most of the oil shale kerogen decomposition reaction rate kinetic data are fitted to a first order model from which the kinetic parameters such as pre-exponential factor and activation energy are calculated. It has been noted that the non-isothermal TGA approach can simulate the conditions in commercial-scale oil shale retorting systems [14].

In order to further optimize the process conditions and retort dimensions, there is a clear need to investigate oil shale pyrolysis kinetics. Analyzing US, Chinese and Estonian oil shale samples can provide answers to whether similar units and/or similar technological processes are applicable to oil shales of varying origin, age and composition. As of today, there are several studies, which have reported wall-to-wall kinetic parameter values (activation energy values from 13 to 215 kJ/mol) for the oil shale decomposition rate reaction [5, 18, 22–24]. Thus this research also aims to offer clarification to the range of kinetic parameter values for oil shale pyrolysis in the temperature range from 300 to 500 °C at modest heating rates.

## 2. Experimental

### 2.1. Materials tested

Oil shale samples used in this investigation were from the subsequent locations and are named in this research as follows: Estonian – from an underground mine called “Estonia” in Estonia; Green River 1 – from the Green River shale formation, Colorado, U.S.A.; Green River 2 – from the Green River shale formation, U.S.A.; Kentucky – from the New Albany shale formation, Kentucky, U.S.A.; Chinese 1 and Chinese 2 – from the Maoming mine, Guangdong Province, Southwest China with the local classifications of C and A, respectively.

All oil shale samples used in pyrolysis tests were previously dried, crushed (if needed) and sieved (1 mm opening). The results of elemental analysis of oil shales tested are given in Table 1.

**Table 1. Elemental analysis results for oil shales tested. All percentages are offered per oil shale mass basis**

Sample	N, %	C <sup>total</sup> , %	H, %	S, %
Estonian	0.0	27.3	2.7	1.5
Green River 1	0.9	27.7	3.2	1.4
Green River 2	0.4	17.2	1.7	0.8
Kentucky	0.5	15.4	1.7	1.8
Chinese 1	0.9	23.3	2.4	2.2
Chinese 2	0.9	23.0	3.0	2.0

## 2.2. Experimental setup and methods applied

The recommendations presented in [25] for collecting experimental thermal analysis data were followed in this study. The kinetics of all oil shale samples was investigated with the NETZSCH STA 449 F3 Jupiter<sup>®</sup> TG-DSC apparatus. In order to avoid mass transfer limitations, a thin layer of  $20 \pm 1$  mg of oil shale was placed into Pt/Rh alloy crucibles with removable thin walled liners of  $\text{Al}_2\text{O}_3$  during the pyrolysis experiments. Oil shale samples were heated from 40 to 950 °C using a linear heating rate of  $20 \text{ °C min}^{-1}$ . A carrier gas flow of 50 ml/min of high purity  $\text{N}_2$  gas was used for all the experiments. Prior to each pyrolysis test the TGA system was flushed with high purity  $\text{N}_2$  gas to remove any residual air. The temperature and enthalpy calibrations of the apparatus were done using In, Sn, Zn, Al and Au standards. In order to eliminate buoyancy effects during the furnace heat-up cycle, empty crucible experiment background mass data were recorded and subtracted from each oil shale measurement data set. Excellent reproducibility (for two or three parallel measurements) was observed for the mass loss curves. All the reported final results are the average values of the conducted repeated measurements.

Characteristic oil shale decomposition temperatures were recorded at the start of thermal decomposition ( $T_s$ ), at the temperature when maximum mass loss rate occurred ( $T_{\max}$ ), and at the end of thermal decomposition ( $T_e$ ).  $T_s$  and  $T_e$  temperatures were set according to the intersection of the tangents and  $T_{\max}$  as the temperature value corresponding to the maximum decomposition rate. These characteristic temperatures can be seen in Figure 1.

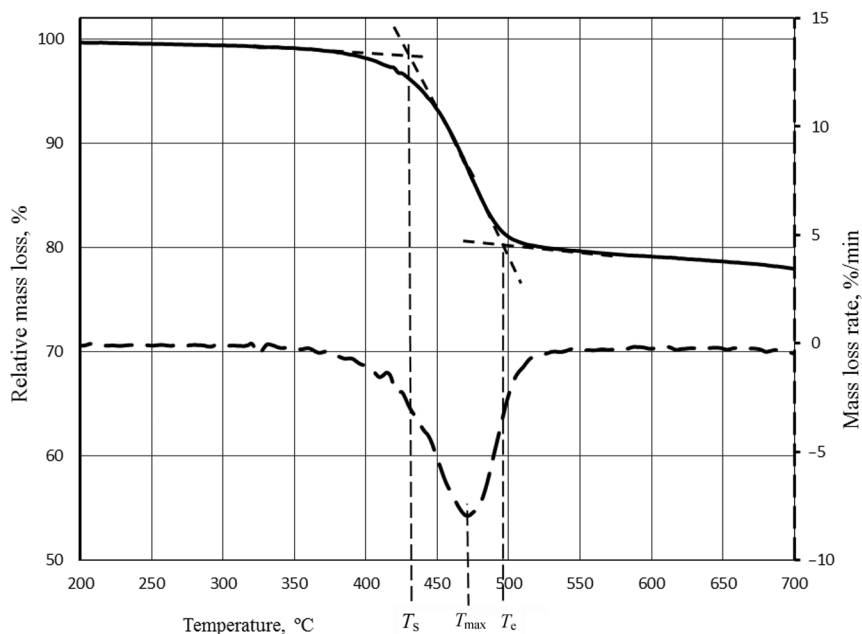
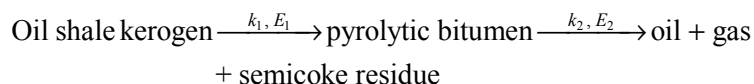


Fig. 1. Characteristic temperatures of an oil shale sample pyrolysis thermogravimetric (TG) profile.

### 2.3. Decomposition reaction kinetic parameters

According to Rajeshwar [15] the general reaction mechanism of oil shale kerogen decomposition is as follows:



In the initial stages of the decomposition process, species with low molecular weight are distilled and in the second step, long hydrocarbon chains are cracked into smaller hydrocarbon molecules [22]. Therefore, during oil shale decomposition the reaction occurs in two zones. This theory is supported by use of mass spectrometry for shale oil compositional measurements [20].

Kinetic parameters such as activation energy and pre-exponential factor of decomposition are often obtained from the decomposition reaction rate expression. The kinetics may be represented as follows [26]:

$$\frac{d\alpha}{dt} = kf(\alpha), \quad (1)$$

where  $\alpha$  is the fraction reacted in time  $t$ ,  $k$  is the rate constant and the function  $f(\alpha)$  depends on the decomposition mechanism. The rate constant  $k$  can be explained by the Arrhenius equation:

$$k = A^* \exp\left(\frac{-E}{RT}\right), \quad (2)$$

where  $A$  is the frequency or pre-exponential factor,  $E$  is the activation energy and  $R$  is the universal gas constant.

The conversion of kerogen to products at any time  $t$  can be defined as fractional weight loss ( $\alpha$ ):

$$\alpha = \frac{W_0 - W_t}{W_0 - W_f}, \quad (3)$$

where  $W_0$  is the initial weight of the sample,  $W_t$  is the weight of the sample at time  $t$  (variable), and  $W_f$  is the final mass at the end of the reaction. Due to the moisture content of some samples, the conversion  $\alpha$  was recalculated to zero at 200 °C, so that the kinetic parameters would only be representative of the pyrolysis of dry kerogen.

The Coats-Redfern integral method was used to determine whether the decomposition involves one or two zones and to obtain the respective activation energy and pre-exponential factor values [15]. Using the Arrhenius equation and combining it with a linear heating rate  $\beta$ , and integrating, one gets [27]:

$$\frac{1-(1-\alpha)^{1-n}}{1-n} = \frac{ART^2}{\alpha E} \left[ 1 - \frac{2RT}{E} \right] \exp\left(-\frac{E}{RT}\right). \quad (4)$$

For the reaction order of  $n = 1$ , Equation 4 can be written as follows:

$$\ln\left[-\frac{\ln(1-\alpha)}{T^2}\right] = \ln\frac{AR}{\beta E} \left[ 1 - \frac{2RT}{E} \right] - \frac{E}{RT}. \quad (5)$$

Therefore, a plot of  $\ln[-\ln(1-\alpha)/T^2]$  vs  $1/T$  should result in a straight line with the slope of  $-E/R$  and an intercept of  $\ln(AR/\beta E)$ . The presence of a ‘breaking point’ in the data confirms that there are two consecutive zones during the decomposition reaction.

The second kinetic analysis method used in this paper was the direct Arrhenius method [15]. When combining the aforementioned decomposition reaction (1) and combining it with the Arrhenius equation (2), in case of a non-isothermal measurement with a linear heating rate ( $\beta$ ), the conversion can be described as:

$$\frac{d\alpha}{dt} = \frac{A}{\beta} \exp\left(-\frac{E}{RT}\right) (1-\alpha)^n. \quad (6)$$

Therefore, in case of  $n = 1$ , a plot of  $\ln[(d\alpha/dT)/(1-\alpha)]$ , also stated as  $\ln k$  vs  $1/T$ , will yield a straight line from which  $E$  and  $A$  can be calculated from the slope and intercept, respectively.

### 3. Results and discussion

#### 3.1. Oil shale organic and mineral contents

Figure 2 shows the weight loss data for the pre-dried samples of American, Chinese and Estonian oil shales as a function of temperature heated with a constant heating rate of  $20\text{ }^\circ\text{C min}^{-1}$  in a  $\text{N}_2$  atmosphere. As can be seen from the figure, all the samples exhibit different mass loss magnitudes. Little if any mass loss below  $200\text{ }^\circ\text{C}$  is assigned to the evaporation of water and is not displayed in Figure 2. Estonian oil shale shows the greatest total mass loss of 47 %, including both organic matter and carbonate part decomposition. The Green River 1 oil shale exhibits a quite similar mass loss profile with a total mass loss of 42%. The Green River 2 sample can be considered somewhat similar to the abovementioned samples, since it shows similar steps but in smaller magnitude – the total mass loss is 35%. The mass losses of Kentucky, Chinese 1 and Chinese 2 oil shale samples are noticeably different from those of the aforesaid samples – these samples have a slightly smaller total mass loss (only up to 28 %). The Chinese 1 sample exhibits carbonate mineral decomposition of about just 6%, however, Chinese 2 and Kentucky oil shales do not seem to contain any carbonate mineral. It is worth noting that the mass loss of Chinese 2 and Kentucky oil shales does

not remain constant (a constant negative slope) during the heating at a temperature beyond 600 °C. This behavior of the sample might be due to the mineral portion reduction during the heating in an inert atmosphere. If compared to the other oil shale samples, Estonian oil shale has the highest carbonate mineral content (22%). As can be also seen from Figure 2 and Table 2, the total extractable kerogen content varies from 12 to 27%, respectively, for the samples of Kentucky and Green River 1.

As seen from the figure, most oil shale powders were dry prior to the analysis. The first mass loss (between 300 and 550 °C) is attributed to the pyrolysis of oil shale in inert N<sub>2</sub> gas atmosphere when heated at 20 °C/min. The second mass loss (between 650 and 850 °C) is ascribed to the decomposition of oil shale carbonates.

Characteristic temperatures for the decomposition reaction for oil shale samples tested are cumulatively shown in Table 2. As can be seen from the table, the Green River 1 oil shale sample exhibits the highest determined temperature values, indicating low kerogen reactivity or delayed decomposition reaction if compared to the other samples. On the contrary, the samples Kentucky and Green River 1 have the most delayed thermal decomposition and therefore the highest temperatures at maximum mass loss rate, although the extent of the reaction (temperature difference between the start and end of thermal decomposition) is the highest. It seems Kentucky oil shale kerogen is most reactive if compared to the rest of oil shales in the sample

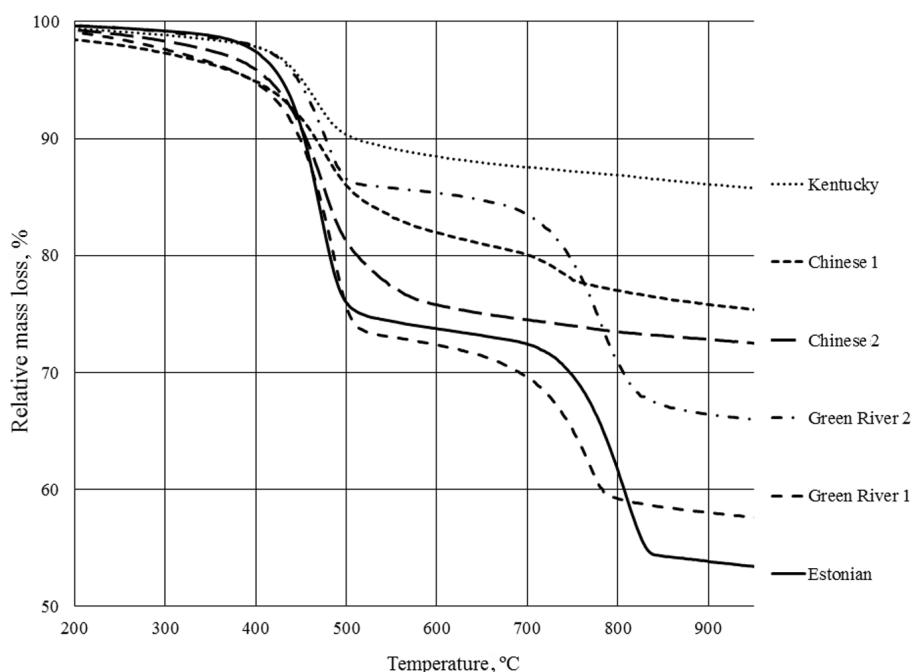


Fig. 2. TG profiles of the analyzed oil shale samples.

**Table 2. Oil shale kerogen and carbonate contents and characteristic temperatures of pyrolysis obtained at the beginning, at the end and at maximum mass loss rate of the reaction**

Result \ Sample	Estonian	Green River 1	Green River 2	Kentucky	Chinese 1	Chinese 2
Residual mass, %	53	58	65	85	75	72
Total mass loss, %	47	42	35	15	25	28
Pyrolysis of organics, %	24	27	14	12	18	24
Fischer assay oil yield, %	17	19	10	8	13	17
Decomposition of carbonate minerals, %	22	14	19	0	6	0
Start of thermal decomposition of kerogen, °C	432	435	434	419	n.d	n.d
Temperature of maximum mass loss speed of kerogen, °C	471	483	476	465	475	473
End of thermal decomposition of kerogen, °C	495	504	498	501	n.d	n.d

\* n.d – not determined due to curve shapes obtained

bank. Estonian and Green River 1 oil shale samples exhibit a higher organic content and a smaller residual mass. This is consistent with the Fischer Assay oil yield results (see results in Table 2), where it is shown that Estonian, Green River 1 and Chinese 2 oil shale samples exhibited the highest oil yields. Fischer Assay oil yield, in percent (%), was calculated from the kerogen content according to Cook [28]. The Fischer Assay oil yields in this study are quite comparable to those presented in the work of Goldfarb et al. [9], except the Estonian oil shale yield. It should be noted that the Estonian oil shale used in [9] was from “Aidu” mine, however, this study employed a sample from “Estonia” mine.

$T_s$  and  $T_e$  temperatures were not determined for Chinese oil shale samples due to the shape of their mass loss curves – in this case the intersection of tangents would not give meaningful temperature values.

As Table 2 shows, the organic content is the highest in Estonian, Green River 1 and Chinese 2 oil shale samples, however, the highest carbonate content is in Estonian and Green River 2 oil shale samples.

The main mass loss occurring at temperatures below around 600 °C is attributed to the decomposition of kerogen present in oil shale [22]. It is known that the pyrolysis process temperature is related to the rate of weight loss, since higher temperatures cause greater weight loss or higher oil yields [14]. In our case, complete decomposition of organics occurs at temperatures up to 550 °C. Above 650 °C, the decomposition of carbonate minerals as well as changes in the chemical structure of clay minerals takes place. As can be seen from the results in Table 2, the mass loss originating from the decomposition of Green River 1 carbonates is smaller than for the decomposition of the same oil shale kerogen. It is interesting that for the Green

River 2 sample, in opposite, the magnitude of kerogen decomposition is smaller than the step of decomposition of carbonates. The temperature values, between which the kerogen decomposition reaction occurs, are about the same for Estonian and both Green River samples. The results in Table 2 also reveal that the organic content is more or less the same for Estonian, Green River 1 and Chinese 2 samples, ranging from 24 to 27%.

Figure 3 depicts the differential TGA rate curves of the analyzed samples. As seen from the graph (and results in Table 2), the maxima of various oil shale decomposition rates are more or less similar ranging from 465 to 483 °C. There seems to be no correlation between the extent of the kerogen decomposition and the temperatures recorded at maximum rate. Although, Chinese 2 and Kentucky oil shales exhibit a continuous very slow mass loss and therefore the differential mass loss curve does not show any peaks. Additionally, it can be seen that the larger the carbonate mineral decomposition step (in %), the more intense the peak and the more delayed the peak maximum. The results in Table 2 demonstrate that the characteristic thermal temperatures of oil shale kerogen decomposition are in more or less the same range, and therefore it seems that the reaction rate is independent of the origin, age and composition of oil shale.

As seen from Figure 3, pyrolysis in all oil shale samples tested begins at around 300 °C, and is over at about 530 °C. Estonian and US Green River 1 are the highest kerogen oil shales. Independent of the origin of oil shale, as expected, the decomposition of carbonate minerals begins at around 650 °C.

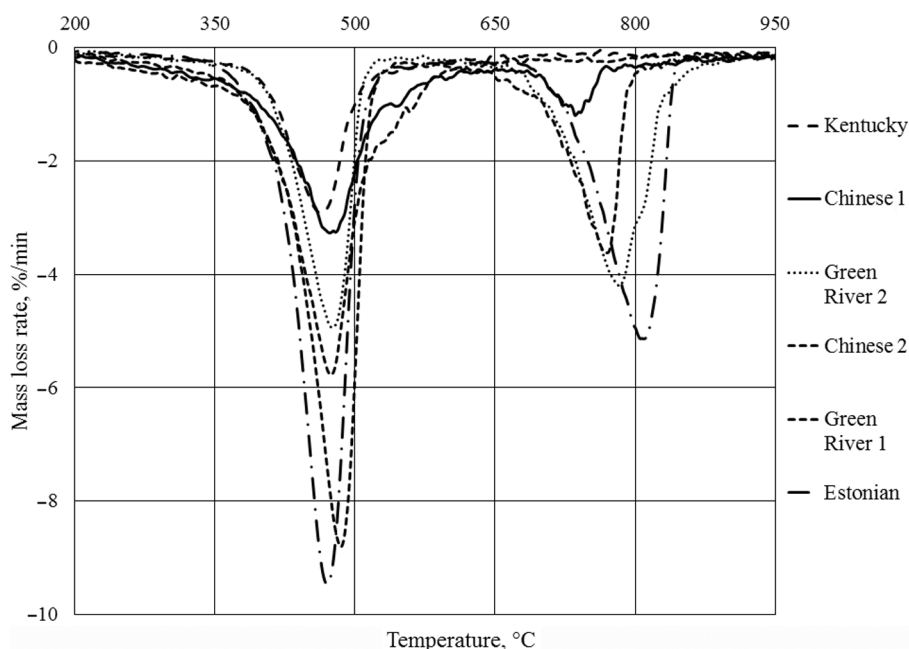


Fig. 3. Differential TG curves of the analyzed oil shale samples.

Estonian, US Green River 2 and US Green River 1 samples have the highest carbonate content.

The assumption of first-order reactions seems reasonable due to uniform Gaussian distribution style differential rate curves (see Fig. 3) for all oil shales. Long tail of the differential rate curve would suggest rate order to be over 1, and long heads of the curve would suggest rate order to be below 1. None of this is the case, and therefore assumption of first order kinetics during decomposition seems reasonable.

As a summary of this section, oil shale samples investigated in this work have different mass loss and differential mass loss rate profiles due to their different origin and composition. However, oil shale kerogen decomposition reaction rates seem to be independent of oil shale origin and composition.

### 3.2. Oil shale decomposition kinetic parameters and their comparison to literature data

As mentioned in the Experimental section, the Coats-Redfern integral and direct Arrhenius plot methods were used to calculate the kinetic rate parameters such as pre-exponential factor and activation energy. Their common advantage is that the presence of a distinct “breaking point” at certain temperatures (see Figs. 4 and 5) in the data plot verifies that there might be two consecutive reaction zones with slightly different temperature ranges. This can be explained as a change in the rate of decomposition at some critical temperature. The difficulties associated with clearly determining this “breaking point” are related to various reactions taking place during oil shale decomposition, which do overlap to some extent and could therefore influence the calculated rate parameters.

Figure 4 represents the direct Arrhenius plot method analysis results. As can be seen from the presented results, the decomposition rate proceeds in two zones where firstly the kerogen decomposes into pyrolytic bitumen, which is then further converted to complicated hydrocarbons with varying length as previously seen in the literature [22, 29]. It should be noted that in the lower temperature zone for each oil shale, the data dispersion is the highest ( $R^2$  values are relatively low) if compared to the second reaction zone. In addition it can be seen from the graph that Estonian oil shale seems to be slightly different from the other samples – the “breaking point” is at a lower temperature.

Figure 4 shows that the uncertainty of kinetic parameter values obtained in the z1 zone is relatively high when the Arrhenius method is applied. The correlation factors in z1 range from 0.66 up to 0.91, however, in the z2 temperature zone the correlation factors are relatively high, ranging from 0.98 up to 0.99, suggesting excellent kinetic parameters for all oil shales tested.

Figure 5 displays the results of the Coats-Redfern integral method – a plot of  $\ln[-\ln(1-\alpha)/T^2]$  vs  $1/T$ . Three of the oil shale samples are depicted – Estonian, Green River 2 and Kentucky, since they all exhibit slightly

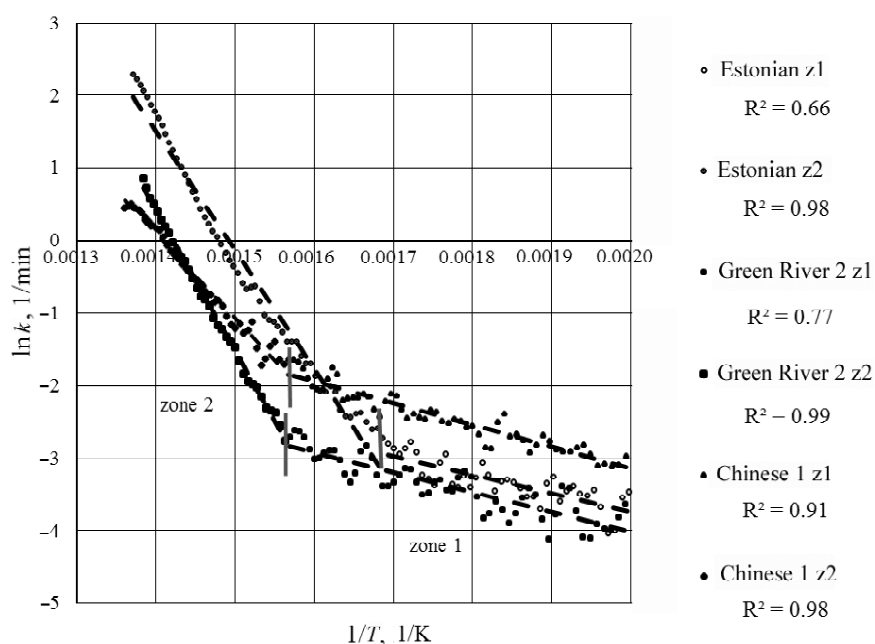


Fig. 4. The direct Arrhenius plot method results for Estonian, US and Chinese oil shale samples, z1 and z2 denoting the reaction zones at lower and higher temperatures, respectively.

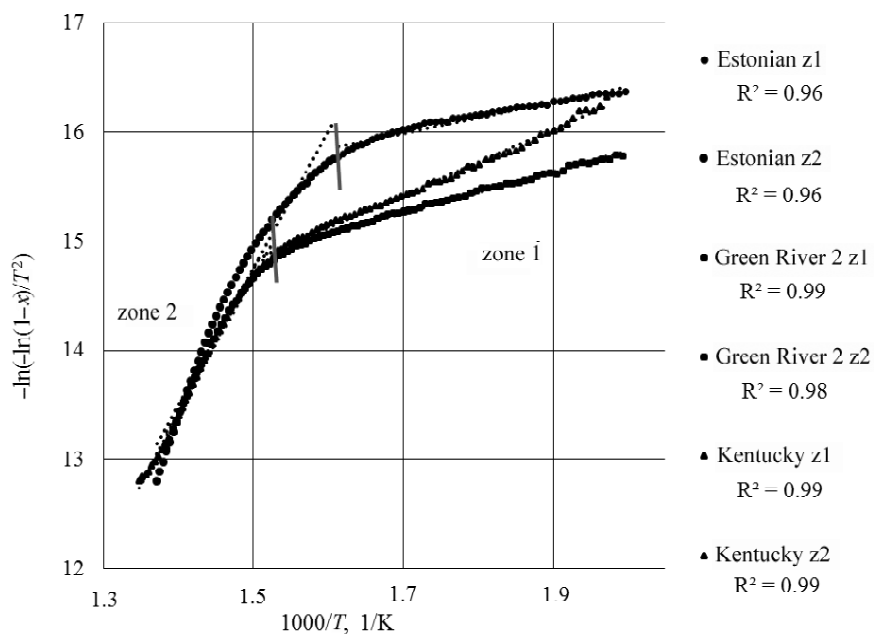


Fig. 5. The Coats-Redfern integral method results for Estonian and US oil shale samples, z1 and z2 denoting the reaction zones of lower and higher temperature range, respectively.

differently shaped rate curves. The other three oil shale data sets show significant overlapping in the two zone “breaking point” temperature region and therefore are not shown. Similarly to the direct Arrhenius method, the results in Figure 5 reveal the existence of two consecutive rate zones during the decomposition reaction. Both zones in Figure 5 are separated with a vertical brown line, which divides “zone 1” and “zone 2” data. The results demonstrate a close linear fitting with  $R^2$  coefficients ranging from 0.96 to 0.99 over the used temperature ranges. Similarly to the results shown in Figure 4 and Figure 5, Estonian oil shale seems to exhibit a higher rate of decomposition. This is due to the higher organic/mineral ratio in oil shale.

Figure 5 shows that the uncertainty of kinetic parameter values obtained in the z1 zone is relatively low, the linear correlation factors range from 0.96 to 0.99. The correlation factors in the z2 temperature zone range from 0.96 up to 0.99, suggesting excellent kinetic parameters for all oil shales tested. It is noticeable that the  $R^2$  values are considerably higher for the Coats-Redfern method (Fig. 5) than for the direct Arrhenius plot method (Fig. 4), which suggests that the Coats-Redfern model fits oil shale decomposition data more precisely than the Arrhenius method. The latter method gives a closer correlation between kinetic parameters in the higher temperature zone (zone 2) in which the cracking of hydrocarbons occurs. It is evident that when using the direct Arrhenius plot method for the lower temperature zone, the correlation coefficients are quite low for Estonian and Green River 2 oil shales. As both of the samples contain about 20% carbonate minerals, the mineral matrix may have a catalytic effect on the on-going reactions in the organic portion. This will be discussed later. For the Estonian oil shale sample, the dispersion of the obtained kinetic parameters is significantly higher than for the other oil shale samples. This might be due to the difference in the composition of oil shale samples, but also possibly due to the different chemical and physical behavior of organic and inorganic portions, since it is not exactly known which chemical or physical changes or molecular rearrangements take place during the heating process.

Qing et al. [29] have reported Chinese Huadian oil shale decomposition kinetics, applying similarly both the direct Arrhenius plot and Coats-Redfern methods. That study shows better rate data correlation with the Arrhenius method, which supports the findings of the current paper. The main difference is that Qing et al. have calculated their kinetic parameters for a single reaction zone, combining all organics decomposition data, but in this research we present activation energy calculations for two reaction zones without eliminating any data points near the breaking point.

The activation energy values calculated both in low and high temperature zones for all oil shales tested are presented in Figure 6. In this figure “zone 1” denotes the lower temperature region reaction zone and “zone 2” the higher temperature region reaction zone.

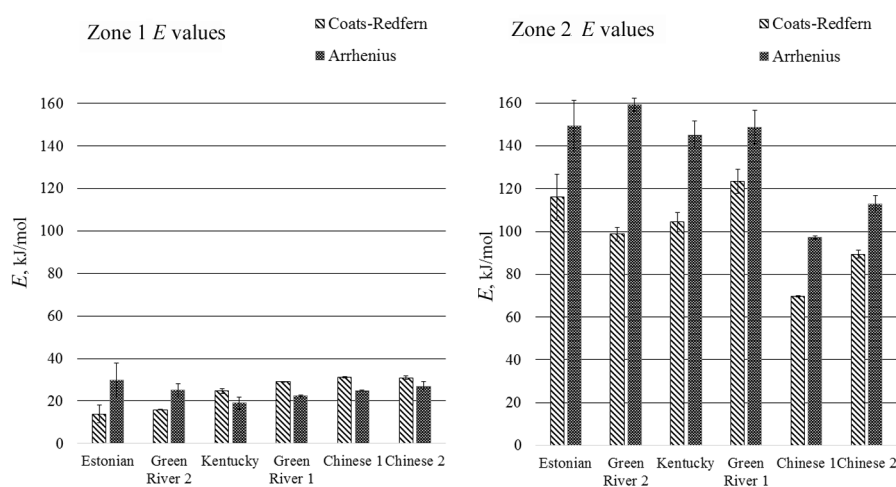


Fig. 6. A comparison of the calculated activation energy values for oil shales tested in two reaction zones.

As seen from the results in Figure 6, independent of the origin of oil shale, the activation energy values in zone 1 are significantly lower, ranging from 14 up to 31 kJ/mol, however, those in zone 2 range from 70 up to 149 kJ/mol. Also, Figure 6 shows that the Coats-Redfern method yields a lower deviation of the obtained kinetic parameter values and a better fit to the data for all oil shales tested, especially for the lower temperature range reaction zone. However, consistently for all oil shales, the direct Arrhenius plot method yields higher activation energy values. An issue that has been discussed in several articles before is the possible catalytic effect of minerals on the pyrolysis of organics in oil shale. It has been shown by Yan et al. [30] that the mineral matrix (mostly carbonates and silicates) in oil shale promotes the decomposition of organic matter during the pyrolysis process – the minerals can affect the organic matter decomposition, and therefore alter kinetic parameter values.

The comparison of activation energy and pre-exponential factor values with the data presented in the literature is shown in Table 3 [12, 31–34]. These results demonstrate that the activation energy values obtained in this work are very similar to those reported by Braun and Rothman (44.6 to 177.6 kJ/mol) for Green River oil shale [31]. The researchers indicated that the activation energy values of the decomposition reaction low temperature zone are lower because of the weaker bonds existing in organics decomposing in the early stages of the process. With the decomposition reaction progressing, the stronger bond organics decompose and the activation energy increases. These results are in correlation with those obtained by Kok and Iscan [23], who reported activation energy calculation for different oil shale samples from Turkey with results falling into the same range. Tiwari and Deo [10] have shown the activation energy values for Green River oil shale

decomposition ranging from 95 to 245 kJ/mol, with uncertainties of about 10%. Liu et al. [13] have calculated the activation energy values for three steps of decomposition of Chinese oil shale samples and obtained the figures in the range of 54 to 277 kJ/mol. The results obtained in this paper are smaller than those reported in the literature. This is not surprising since the samples have different origins and are found in different geological environments.

**Table 3. A comparison of the obtained activation energy values with literature data**

Zone 1	Coats-Redfern method		Direct Arrhenius plot method		Literature data	Reference
Sample	$E_a$ , kJ/mol	$\log A$	$E_a$ , kJ/mol	$\log A$	$E_a$ , kJ/mol	No
Estonian	13.9	10.33	29.8	2.52	31.0	[33]
Green River 1	29.0	8.98	22.5	2.51	44.6	[31]
Green River 2	15.9	9.86	25.1	2.05	50.7 <sup>x</sup>	[34]
Kentucky	24.7	9.30	19.0	1.43	–	–
Chinese 1	31.2	8.72	24.9	2.48	–	–
Chinese 2	30.9	4.92	26.8	2.70	54.0	[12]
Zone 2	Coats-Redfern method		Direct Arrhenius plot method		Literature data	Reference
Sample	$E_a$ , kJ/mol	$\log A$	$E_a$ , kJ/mol	$\log A$	$E_a$ , kJ/mol	No
Estonian	115.9	3.13	149.3	12.43	–	–
Green River 1	123.4	2.61	148.7	12.41	177.6	[31]
Green River 2	98.9	4.26	159.3	12.70	–	–
Kentucky	104.4	3.84	145.1	11.49	211–226 <sup>y</sup>	[32]
Chinese 1	69.7	6.16	97.2	8.21	–	–
Chinese 2	89.4	5.25	112.8	9.66	277.0	[12]

<sup>x</sup> – calculated using different heating rates, <sup>y</sup> – total mean value

As the table shows, the zone 1 activation energy values obtained in this research are in good agreement with the literature data, however, the activation energy values for zone 2 reported in this paper are somewhat lower than the ones published previously.

The kinetic parameter values presented above could potentially differ if common catalysts were eliminated from oil shale prior to its pyrolysis experiment. In this study, we did not eliminate the mineral part prior to the pyrolysis and therefore, our kinetic parameter values represent kinetics with potential catalytic effects. As evidenced from the results presented in Table 3, the activation energy of Kentucky oil shale (which contains no carbonate minerals) has no clear trend if compared to that of Green River 1 (14% carbonates). However, it has been reported that carbonate minerals provide a catalytic effect on pyrolysis kinetics and thereby, lower the

activation energy [22]. In our investigations, such a clear catalytic effect of the carbonate part has not been observed. According to Rajeshwar [15], there should not be any difference in the calculated kinetic parameter values depending on whether kerogen was previously extracted from oil shale or not. Another study has reported that when oil shale vs pure kerogen decomposition TGA curves are compared at different heating rates, the decomposition of oil shale is faster if compared to pure kerogen decomposition, suggesting catalytic effects of minerals present in oil shale [22]. However, Aboulkas and El Harfi [18] observed delayed kinetics for oil shale if compared to the kinetics of pure kerogen. As stated by Al-Harashseh et al. [22], the minerals could offer catalytic effects and therefore enhance heat transfer in oil shale particles, thereby increasing the cracking during pyrolysis. Further study is needed to investigate the catalytic effects of minerals present in oil shale on its pyrolysis kinetics.

The oil shale pyrolysis kinetic parameter values obtained in this investigation were more or less the same for all oil shales tested in either decomposition temperature zone if a heating rate of  $20\text{ }^{\circ}\text{C min}^{-1}$  was applied. Indeed, altering the heating rate might somewhat provide different kinetic parameter values, however, more practical use heating rates (such as in an actual oil shale retort) cannot be obtained with the conventional TGA method. Further study is required to investigate the effect of heating rates applied (heating rates which are more comparable to those of the actual retort process) on oil shale decomposition kinetics.

#### 4. Conclusions

This paper offers the results of the pyrolysis kinetics of American, Chinese and Estonian oil shales applying TGA. The oil shales tested exhibited dissimilar thermal decomposition extents depending on their kerogen content. The activation energy and pre-exponential factor values were obtained applying the direct Arrhenius plot and Coats-Redfern integral methods. Independent of the origin of oil shale the decomposition of kerogen portion proceeds in two temperature zones – in the low temperature zone (kerogen decomposition to bitumen), and in the consequent high temperature zone (a cracking step and the formation of various hydrocarbons). As evidenced from the presented results, both temperature zones exhibit considerably dissimilar activation energy and pre-exponential factor values. There were no clear relationships between the kinetic parameter values recorded if the results from two methods were compared. The Arrhenius plot method yielded the activation energy values in the range of 19 to 30 kJ/mol and 97 to 159 kJ/mol, respectively, for the two occurring temperature zones. The respective figures for the Coats-Redfern integral method were in the range of 14 to 31 kJ/mol and 70 to 116 kJ/mol.

## Acknowledgements

This research was supported by the European Union through the European Regional Development Fund.

## REFERENCES

1. Siirde, A. Oil shale – global solution or part of the problem? *Oil Shale*, 2008, **25**(2), 201–202.
2. Altun, N. E., Hicyilmaz, C., Hwang, J.-Y., Bagci, A. S., K k, M. Oil shales in the world and Turkey; reserves, current situation and future prospects: a review. *Oil Shale*, 2006, **23**(3), 211–227.
3. Konist, A., Loo, L., Valtsev, A., Maaten, B., Siirde, A., Neshumayev, D., Pihu, T. Calculation of the amount of Estonian oil shale products from combustion in regular and oxy-fuel mode in a CFB boiler. *Oil Shale*, 2014, **31**(3), 211–224.
4. Konist, A., Valtsev, A., Loo, L., Pihu, T., Liira, M., Kirsim e, K. Influence of oxy-fuel combustion of Ca-rich oil shale fuel on carbonate stability and ash composition. *Fuel*, 2015, **139**, 671–677.
5. Torrente, M. C., Gal n, M. C. Kinetics of the thermal decomposition of oil shale from Puertollano (Spain). *Fuel*, 2001, **80**(3), 327–334.
6. Lille,  . Current knowledge on the origin and structure of Estonian kukersite kerogen. *Oil Shale*, 2003, **20**(3), 253–263.
7. Hutton, A., Bharati, S., Robl, T. Chemical and petrographic classification of kerogen/macerals. *Energ. Fuel.*, 1994, **8**(6), 1478–1488.
8. Yan, F., Song, Y. Properties estimation of main oil shale in China. *Energ. Source. Part A*, 2009, **31**(4), 372–376.
9. K laots, I., Goldfarb, J. L., Suuberg, E. M. Characterization of Chinese, American and Estonian oil shale semicokes and their sorptive potential. *Fuel*, 2010, **89**(11), 3300–3306.
10. Tiwari, P., Deo, M. Detailed kinetic analysis of oil shale pyrolysis TGA data. *AIChE J.*, 2012, **58**(2), 505–515.
11. Wang, Z., Deng, S., Gu, Q., Zhang, Y., Cui, X., Wang, H. Pyrolysis kinetic study of Huadian oil shale, spent oil shale and their mixtures by thermogravimetric analysis. *Fuel Process. Technol.*, 2013, **110**, 103–108.
12. Bai, F., Sun, Y., Liu, Y., Liu, B., Guo, M., L , X., Guo, W., Li, Q., Hou, C., Wang, Q. Kinetic investigation on partially oxidized Huadian oil shale by thermogravimetric analysis. *Oil Shale*, 2014, **31**(4), 377–393.
13. Liu, Q. Q., Han, X. X., Li, Q. Y., Huang, Y. R., Jiang, X. M. TG–DSC analysis of pyrolysis process of two Chinese oil shales. *J. Therm. Anal. Calorim.*, 2014, **116**(1), 511–517.
14. Jaber, J. O., Probert, S. D. Non-isothermal thermogravimetry and decomposition kinetics of two Jordanian oil shales under different processing conditions. *Fuel Process. Technol.*, 2000, **63**(1), 57–70.
15. Rajeshwar, K. The kinetics of the thermal decomposition of Green River oil shale kerogen by non-isothermal thermogravimetry. *Thermochim. Acta*, 1981, **45**(3), 253–263.
16. Williams, P. T., Ahmad, N. Investigation of oil-shale pyrolysis processing conditions using thermogravimetric analysis. *Appl. Energ.*, 2000, **66**(2), 113–133.

17. Fang-Fang, X., Ze, W., Wei-Gang, L., Wen-Li, S. Study on thermal conversion of Huadian oil shale under N<sub>2</sub> and CO<sub>2</sub> atmospheres. *Oil Shale*, 2010, **27**(4), 309–320.
18. Aboulkas, A., El Harfi, K. Study of the kinetics and mechanisms of thermal decomposition of Moroccan Tarfaya oil shale and its kerogen. *Oil Shale*, 2008, **25**(4), 426–443.
19. Thakur, D. S., Nuttall, H. E., Cha, C. Y. The kinetics of the thermal decomposition of Moroccan oil shale by thermogravimetry. *Prepr. Pap. Am. Chem. Soc., Div. Fuel Chem.*, 1982, **27**, 131–142.
20. Tiwari, P., Deo, M. Compositional and kinetic analysis of oil shale pyrolysis using TGA–MS. *Fuel*, 2012, **94**, 333–341.
21. Zanoni, M. A. B., Massard, H., Martins, M. F., Salvador, S. Application of inverse problem and thermogravimetry to determine the kinetics of oil shale pyrolysis. *High Temp.-High Press.*, 2012, **41**(3), 197–213.
22. Al-Harashsheh, M., Al-Ayed, O., Robinson, J., Kingman, S., Al-Harashsheh, A., Tarawneh, K., Saeid, A., Barranco, R. Effect of demineralization and heating rate on the pyrolysis kinetics of Jordanian oil shales. *Fuel Process. Technol.*, 2011, **92**(9), 1805–1811.
23. K k, M. V., Iscan, A. G. Oil shale kinetics by differential methods. *J. Therm. Anal. Calorim.*, 2007, **88**(3), 657–661.
24. Wang, C., Zhang, X., Liu, Y., Che, D. Pyrolysis and combustion characteristics of coals in oxyfuel combustion. *Appl. Energ.*, 2012, **97**, 264–273.
25. Vyazovkin, S., Chrissafis, K., Di Lorenzo, M. L., Koga, N., Pijolat, M., Roduit, B., Sbirrazzuoli, N., Su ol, J. J. ICTAC Kinetics Committee recommendations for collecting experimental thermal analysis data for kinetic computations. *Thermochim. Acta*, 2014, **590**, 1–23.
26. Jacobs, P. W. M., Tompkins, F. C. Classification and theory of solid reactions. In: *Chemistry of the Solid State* (Garner, W. E., ed.). Butterworths, London, 1955, 184–212.
27. Coats, A. W., Redfern, J. P. Kinetic parameters from thermogravimetric data. *Nature*, 1964, **201**, 68–69.
28. Cook, E. W. Oil-shale technology in the USA. *Fuel*, 1974, **53**(3), 146–151.
29. Qing, W., Baizhong, S., Aijuan, H., Jingru, B., Shaohua, L. Pyrolysis characteristics of Huadian oil shales. *Oil Shale*, 2007, **24**(2) 147–157.
30. Yan, J., Jiang, X., Han, X., Liu, J. A TG-FTIR investigation to the catalytic effect of mineral matrix in oil shale on the pyrolysis and combustion of kerogen. *Fuel*, 2013, **104**, 307–317.
31. Braun, R. L., Rothman, A. J. Oil-shale pyrolysis: kinetics and mechanism of oil production. *Fuel*, 1975, **54**(2), 129–131.
32. Knauss, K. G., Copenhaver, S. A., Braun, R. L., Burnham, A. Hydrous pyrolysis of New Albany and Phosphoria shales: production kinetics of carboxylic acids and light hydrocarbons and interactions between the inorganic and organic chemical systems. *Org. Geochem.*, 1997, **27**(7–8), 477–496.
33. Ots, A. *Oil Shale Fuel Combustion*. Tallinna Raamatutr kikoda, 2006.
34. Schenk, H. J., Dieckmann, V. Prediction of petroleum formation: the influence of laboratory heating rates on kinetic parameters and geological extrapolations. *Mar. Petrol. Geol.*, 2004, **21**(1), 79–95.

Presented by A. Siirde and O. Trass

Received November 30, 2015